Wang *et al.*
Chinese Journal of Mechanical Engineering (2023) 36:130
https://doi.org/10.1186/s10033-023-00954-x

Chinese Journal of Mechanical Engineering

ORIGINAL ARTICLE

Open Access

Prediction and Verification of Forming Limit Diagrams Based on a Modified Shear Failure Criterion

Haibo Wang[1*], Zipeng Wang[1], Yu Yan[1] and Yuanhui Xu[1]

Abstract

The forming limit diagram plays an important role in predicting the forming limit of sheet metals. Previous studies have shown that, the method to construct the forming limit diagram based on instability theory of the original shear failure criterion is effective and simple. The original shear instability criterion can accurately predict the left area of the forming limit diagram but not the right area. In this study, in order to improve the accuracy of the original shear failure criterion, a modified shear failure criterion was proposed based on in-depth analysis of the original shear failure criterion. The detailed improvement strategies of the shear failure criterion and the complete calculation process are given. Based on the modified shear failure criterion and different constitutive equations, the theoretical forming limit of TRIP780 steel and 5754O aluminum alloy sheet metals are calculated. By comparing the theoretical and experimental results, it is shown that proposed modified shear failure criterion can predict the right area of forming limit more reasonably than the original shear failure criterion. The effect of the pre-strain and constitutive equation on the forming limits are also analyzed in depth. The modified shear failure criterion proposed in this study provides an alternative and reliable method to predict forming limit of sheet metals.

Keywords Modified shear failure criterion, Sheet metal forming, Forming limit diagram, Loading path

1 Introduction

Forming limit is the maximum deformation that sheet metals can reach under tensile deformation process. Forming limit diagram (FLD) is an important method to predict the maximum deformation and failure moments in sheet metals deformation processes. It is the most visual, effective, and widely used evaluation method in the study of sheet metals formability [1].

With the development of the computer technology and the finite element method, the sheet metal forming limit research has made some achievements in the theoretical and experimental aspects. But the FLD established with critical strain is not convenient in the actual engineering applications due to the influences of the material parameters and experiment condition. There isn't a perfect experiment method to get the exact FLD of materials. Meanwhile, the experimental method to obtain the FLD is difficult and time consuming. The FLD defined by standard experiments is usually obtained under linear or approximate linear strain paths [2]. But in the actual manufacture processes, the strain paths often deviate from the linear path and the FLD established under simple strain path cannot accurately predict the failure occurrence. Therefore, it is necessary to adopt an appropriate sheet metal forming failure criterion to construct the FLD, which is established under complicated strain paths that are generally in accordance with the actual forming processes. The researches on the influences of the FLD under complicated strain paths are the main research content of the sheet metal forming field so far.

*Correspondence:
Haibo Wang
wanghaibo@ncut.edu.cn
[1] School of Mechanical and Materials Engineering, North China University of Technology, Beijing 100144, China

Springer Open

© The Author(s) 2023. **Open Access** This article is licensed under a Creative Commons Attribution 4.0 International License, which permits use, sharing, adaptation, distribution and reproduction in any medium or format, as long as you give appropriate credit to the original author(s) and the source, provide a link to the Creative Commons licence, and indicate if changes were made. The images or other third party material in this article are included in the article's Creative Commons licence, unless indicated otherwise in a credit line to the material. If material is not included in the article's Creative Commons licence and your intended use is not permitted by statutory regulation or exceeds the permitted use, you will need to obtain permission directly from the copyright holder. To view a copy of this licence, visit http://creativecommons.org/licenses/by/4.0/.

The theoretical basis of the FLD prediction is the tensile instability theory and there are many methods to predict FLD. The earliest theories still used are the Hill centralized instability theory [3] and Swift scattered instability theory [4]. The most widely used instability theory is M-K groove theory [5], which is a famous non-uniform assumption theory. S-R theory is lack of the experimental evidence of the existence of the sharp point on the yield surface, so it is not widely accepted. The C-H instability model proposed by Chen et al. [6] is a plane strain instability shifting model.

These instability theories above have some problems more or less. In Hill centralized instability theory, there isn't a zero-strain line under biaxial tensile condition. Therefore, the centralized instability will confine the deformation amount. In Swift scattered instability theory, the simple loading condition is required but it is only applicable in equal biaxial tensile condition, which limits its application. In M-K groove theory, a non-uniform degree of initial thickness needs to be given. S-R theory is lack of the experimental evidence of the existence of the sharp point on the yield surface, so it is not widely accepted.

Since 2011, Huang and Chen [2] analyzed the progresses on fracture criterion of sheet metal forming. Regarding that the shear failure of AHSS before necking, the failure mechanism was still immature and needed to be further elucidated to improve the forming quality of AHSS. In 2013, Bjorklund et al. [7] explored the failure of the high strength steel Docol 600DP and the ultra-high strength steel Docol 1200M, which used plastic anisotropy and mixed isotropic kinematic hardening. However, the shear fracture was not predicted with a satisfying result by the Bressan-Williams model, and further studies were needed to improve these predictions. In 2014, A macroscopic ductile fracture criterion was proposed by Lou et al. [8] based on micro-mechanism analysis of nucleation, growth and shear coalescence of voids from experimental observation of fracture surfaces to construct fracture loci of AA2024-T351 and got a satisfactory prediction compared with experimental results. In 2017, Park et al. [9] was concerned with modeling of fracture-based forming limit criteria for anisotropic materials in sheet metal forming to predict the sudden fracture in complicated forming processes. Three different kinds of fracture-based forming limit criteria were suggested and investigated with an assumption that the stress state was under the plane stress condition with proportional loading. In 2017, Rajdeep and Park [10] presented a numerical model to predict flow-induced shear failure along pre-existing fractures. In 2018, Li et al. [11] proposed a general instability criterion, which considered the effects of rate sensitivity, strain hardening and heat softening on the instability behavior of the material and showed the effects of stress loading, strain rate sensitivity and heat conduction on heat softening. In addition, this criterion was illustrated by the instability phase diagram. The analysis results revealed the pressure-sensitive property of shear zone instability.

In 2019, Lou et al. [12] developed an anisotropic ductile fracture criterion by introducing anisotropic parameters into the weight function of an uncoupled shear ductile fracture criterion. The proposed anisotropic ductile fracture was applied to describe the anisotropic characteristics in the ductile fracture of AA6082-T6. In 2020, Lou et al. [13] proposed a yield function to model sheet metal strength between shear and plane strain tension, which was expressed as an equation of the three stress invariants to take into account the pressure sensitivity, the Lode dependence and the strength-differential effect on material strength. Then experiments were conducted with designed specimens to characterize the mechanical behavior of AA7075 and QP980 sheet between shear and plane strain tension. In 2021, Lou et al. [14] introduced a user-friendly approach to model loading direction effect on fracture limits of sheet metals. The approach was combined with a newly developed fracture criterion to illustrate anisotropic fracture in shear, uniaxial tension and plane strain tension as well as fracture under balanced biaxial tension.

In 2011, Lin et al. [15] proposed the original shear failure criterion, an easily used criterion. The trend of right part of the FLC was rising constantly under this criterion. However, according to the right part of experimental FLD, the trends of FLC should rise firstly then decrease. Hence the original shear failure criterion will not be appropriate for the latter kinds of materials. In order to improve the accuracy and enlarge application scope of the original shear failure criterion, a new method called modified shear failure criterion to predict the right part of the FLD is proposed in this study, which is verified by comparing with the experimental data.

The analysis of the maximum shear stress will be discussed in this study, and the study is organized as follows. In Section 2, a new method for calculating maximum shear stress was proposed, which can be used to calculate both right and left parts of FLD and has been named as 'modified shear failure criterion'. In order to validate the modified shear failure criterion, Hill48 yield function and several constitutive equations were adopted which are presented in Section 3 and Section 4. In addition, a general flow diagram about calculating FLD was arranged in Section 4; Trip780 steel and 5754O aluminum alloy sheets were adopted to validate the failure model. Finally, the FLD calculated with the modified shear failure

criterion is discussed in comparison with the experimental results.

2 Theoretical Basis

2.1 Original Shear Failure Criterion

In the original shear failure criterion, a maximum shear stress is assumed to exist in the sheet metal tensile process [15]. If the shear stress is larger than the critical value τ_{cr}, namely,

$$\tau \geq \tau_{cr}. \tag{1}$$

The material will fail and the maximum shear stress equation is:

$$\tau = \frac{1}{2}(\sigma_1 - \sigma_2). \tag{2}$$

The constitutive equation and yield criterion equation have been selected. σ_1, σ_2 are the major principal stress and the minor principal stress respectively. This theory is also called "The maximum shear stress theory" or "The third strength theory". However, Eq. (2) has some complicated factors, such as the sequence of principal stresses which will change accidently with the loading conditions. Due to the existence of anisotropic and strain ratio of the sheet metal, the angle between the direction of the maximum shear stress plane and the direction of the maximum principal strain is not always 30°, so the shear failure will happen on a special shear face. With the direction cosine n_1, n_2, n_3 of the plane, the normal stress σ_n, Eq. (3) and the shear stress τ, Eq. (4) of this plane can be obtained:

$$\sigma_n = \sigma_{11}n_1^2 + \sigma_{22}n_2^2 + \sigma_{33}n_3^2 + \sigma_{12}n_1n_2 + \sigma_{13}n_1n_3 + \sigma_{23}n_2n_3, \tag{3}$$

$$\tau = \sqrt{(\sigma_{11}n_1 + \sigma_{12}n_2 + \sigma_{13}n_3)^2 + (\sigma_{21}n_1 + \sigma_{22}n_2 + \sigma_{23}n_3)^2 + (\sigma_{31}n_1 + \sigma_{32}n_2 + \sigma_{33}n_3)^2 - \sigma_n^2}. \tag{4}$$

The critical shear stress of the forming process depends on the plastic strain increment. The material will fail when $\tau \geq \tau_{cr}$, so it is important to determine the directional cosine of the plane. The directional cosine is determined with the two angles (φ, θ) which are used to define the maximum shear stress plane, as shown in Figure 1. Number 1 at the bottom represents the direction of the first principal stress, Number 2 represents the direction of the second principal stress, and Number 3 represents the thickness direction. The directional cosine of the plane can be (n_1, n_2, n_3).

$$n_1 = \cos\theta \sin\varphi,\ n_2 = \cos\varphi,\ n_3 = \sin\theta \sin\varphi. \tag{5}$$

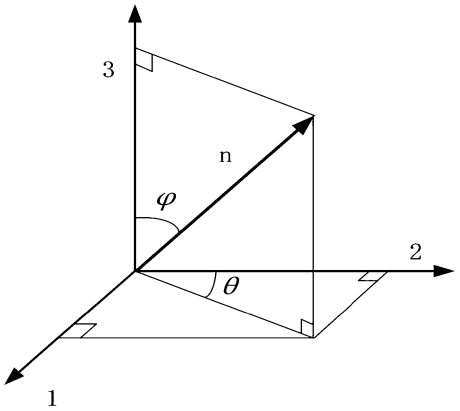

Figure 1 Maximum shear stress plane with (φ, θ)

The sheet metal deforms under the first principal stress and the zero-strain line will occur on the right part of the FLD in biaxial tensile. The angle φ is the default value $\varphi = \pi/2$ in the original shear failure criterion, but the default unchanged value will lead to subjectivity in the predicted result. In order to improve the applicability, a new calculation method, namely, the modified shear failure criterion is proposed in this paper. The calculation method of angle θ is the same as the original method, but the value of φ is not the default value $\pi/2$, which will be explained in detail later.

Herein define a ratio β to calculate the two angels (φ, θ), which is the ratio of the strain increments. The range of the strain increment ratios is from 0.5 to 1.

$$\beta = \frac{d\varepsilon_2}{d\varepsilon_1}. \tag{6}$$

Therefore, the magnitude of $d\varepsilon_2$ value determine which plane has the pure shear stress. In addition, shear failure will occur in one special shear plane due to any point in the deformation region. The stress state can be written as:

$$\sigma = \begin{bmatrix} \sigma_{11} & \sigma_{12} & \sigma_{13} \\ \sigma_{21} & \sigma_{22} & \sigma_{23} \\ \sigma_{31} & \sigma_{32} & \sigma_{33} \end{bmatrix}. \tag{7}$$

Under the plane stress and principal stress space condition, the stress tensor can be expressed as:

$$\sigma = \begin{bmatrix} \sigma_{11} & 0 & 0 \\ 0 & \sigma_{22} & 0 \\ 0 & 0 & 0 \end{bmatrix}. \tag{8}$$

2.2 Modified Shear Failure Criterion

Based on the original shear failure criterion proposed by Lin et al. [15], the modified shear failure criterion is proposed in this part. In addition, the values of (φ, θ), β and $d\varepsilon_2$ are needed for this criterion. There would be two cases of shear failure plane-stress condition for numerical magnitude of $d\varepsilon_2$.

Condition 1: $(d\varepsilon_2 \geq 0)$

In the right part of the FLD, $d\varepsilon_2 \geq 0$ and $\varphi = \pi/2$. On the theoretical basis of modified shear failure criterion, the mathematic expression of the directional cosine of stress, (n_1, n_2, n_3) is not changed like Eq. (5). The projection length of Direction 1 (as shown in Figure 1) is $\cos\theta \sin\varphi$ and the projection length of thickness direction is $\sin\theta \sin\varphi$. The directional cosine of plane 1-2 is:

$$\left(\frac{\cos\varphi}{\sqrt{\cos^2\varphi + \cos^2\theta \sin^2\varphi}}, \frac{\cos\theta \sin\varphi}{\sqrt{\cos^2\varphi + \cos^2\theta \sin^2\varphi}} \right). \tag{9}$$

The directional cosine of plane 1-3 is:

$$\left(\frac{\cos\theta \sin\varphi}{\sqrt{(\cos\theta \sin\varphi)^2 + (\sin\theta \sin\varphi)^2}}, \frac{\sin\theta \sin\varphi}{\sqrt{(\cos\theta \sin\varphi)^2 + (\sin\theta \sin\varphi)^2}} \right). \tag{10}$$

After simplification, its result is $(\cos\theta,\ \sin\theta)$. Moreover, the equations need to be satisfied for Plane 1-2 and Plane 1-3:

$$\Delta\varepsilon_1 \frac{\cos^2\varphi}{\cos^2\varphi + \cos^2\theta \sin^2\varphi} + \Delta\varepsilon_2 \frac{\cos^2\theta \sin^2\varphi}{\cos^2\varphi + \cos^2\theta \sin^2\varphi} = 0, \tag{11}$$

$$\Delta\varepsilon_1 \sin^2\theta + \Delta\varepsilon_3 \cos^2\theta = 0. \tag{12}$$

Therefore (φ, θ) is given as follows. In addition, here defines $\tilde{\varepsilon}_2$. The relationship between (φ, θ) and $(\Delta\varepsilon_1,\ \Delta\varepsilon_2,\ \Delta\varepsilon_3)$ is given by:

$$\tan^2\theta = \frac{\Delta\varepsilon_1}{\Delta\varepsilon_3}, \tag{13}$$

$$\tan^2\varphi = \frac{\Delta\varepsilon_1}{\Delta\tilde{\varepsilon}_2}, \tag{14}$$

$$\tilde{\varepsilon}_2 = -\frac{\Delta\varepsilon_3}{\Delta\varepsilon_1 - \Delta\varepsilon_3}\Delta\varepsilon_2, \tag{15}$$

$$2\theta = \arccos\left(\frac{\Delta\varepsilon_1 + \Delta\varepsilon_3}{\Delta\varepsilon_1 - \Delta\varepsilon_3} \right), \tag{16}$$

$$\varphi = \arccos\left(\frac{\Delta\varepsilon_2 - \Delta\varepsilon_1 + \Delta\varepsilon_3}{\Delta\varepsilon_2 + \Delta\varepsilon_1 - \Delta\varepsilon_3} \right). \tag{17}$$

The values of (θ, φ) can be solved by using above method. Finally, according to Eq. (3) and Eq. (4), the angles calculated were substituted into the shear stress calculation equation to obtain the maximum shear stress.

Condition 2: $(d\varepsilon_2 \leq 0)$

In the left part of the FLD, $d\varepsilon_2 \leq 0$ and $\varphi \neq \pi/2$ which is different from the φ in the theory of the original shear failure criterion. Similarly, the directional cosine is also $(n_1, n_2, n_3) = (\cos\theta \sin\varphi,\ \cos\varphi,\ \sin\theta \sin\varphi)$.

Then substitute it into Eq. (11) and Eq. (12) to obtain the relation of (θ, φ). The calculation method of θ is not changed, but φ is changed and given by the following Eq. (18). According to Eq. (3) and Eq. (4), getting the maximum shear stress that is as Eq. (19):

$$2\varphi = \arccos\left(\frac{\Delta\varepsilon_1 + \Delta\tilde{\varepsilon}_2}{\Delta\tilde{\varepsilon}_2 - \Delta\varepsilon_1} \right), \tag{18}$$

$$\tau = \sqrt{\sigma_{11}\left(n_1^2 - n_1^4\right) + \sigma_{22}\left(n_2^2 - n_2^4\right) - 2\sigma_{11}\sigma_{22}n_1^2n_2^2}. \tag{19}$$

The values of (θ, φ) under different conditions can be solved with the above method. If the shear stress is larger than the limit, the material will fail.

3 Yield Criterion

In this study, the Hill48 yield criterion (Hill, 1948) were employed to describe the stress of the yield loci [16, 17]. Yield criterion means under certain deformation condition (deformation temperature, deformation speed, etc.), the material enters plastic deformation state only when the stress components conform to certain relations. The equation of Hill48 criterion under plane stress state is shown in Eq. (20):

$$f = (G + H)\sigma_1^2 - 2H\sigma_1\sigma_2 + (H + F)\sigma_2^2 + 2N\sigma_{12}^2. \tag{20}$$

In this equation, F, G, H and N are the anisotropic parameters of the yield criterion, which are determined with the experiment result of different materials. When $3F = 3G = 3H = N$, this yield criterion will turn to the isotropic yield criterion, Mises criterion. There are two methods to calculate the anisotropic parameters of

Hill48 yield criterion. The stress method is shown from Eqs. (21, 22, 23, 24), where σ_0, σ_{45}, σ_{90}, σ_b are the initial yield stresses [18]. σ_0 represents the stress along the rolling direction. σ_{45}, σ_{90} represents the stresses at 45° and 90° to the rolling direction, respectively. σ_{b} represents the biaxial yield stress obtained by the biaxial tensile test. The r-value method is shown from Eqs. (25, 26, 27, 28) where r_0, r_{45}, r_{90} represent the anisotropy parameters for different directions [19].

$$F = \frac{1}{2}\left(\left(\frac{\sigma_0}{\sigma_{90}}\right)^2 - 1 + \left(\frac{\sigma_0}{\sigma_b}\right)^2\right), \tag{21}$$

$$G = \frac{1}{2}\left(1 - \left(\frac{\sigma_0}{\sigma_{90}}\right)^2 + \left(\frac{\sigma_0}{\sigma_b}\right)^2\right), \tag{22}$$

$$H = \frac{1}{2}\left(1 + \left(\frac{\sigma_0}{\sigma_{90}}\right)^2 - \left(\frac{\sigma_0}{\sigma_b}\right)^2\right), \tag{23}$$

$$N = \frac{1}{2}\left(\left(\frac{2\sigma_0}{\sigma_{45}}\right)^2 - \left(\frac{\sigma_0}{\sigma_b}\right)^2\right), \tag{24}$$

$$F = \frac{r_0}{(1+r_0)r_{90}}, \tag{25}$$

$$G = \frac{1}{(1+r_0)}, \tag{26}$$

$$H = \frac{r_0}{(1+r_0)}, \tag{27}$$

$$N = \frac{(1+r_{45})(r_0+r_{90})}{2(1+r_0)r_{90}}. \tag{28}$$

4 Verification of the FLD

4.1 Calculation Process

The method of solving the theoretical forming limit curve makes use of the strain of initial Direction 1 and the ranges of the strain ratio β between Direction 2 and Direction 1. The maximum shear stress angles of material forming limit is calculated under different strain ratios with Eqs. (3) and (4). For the purpose of coincide between the lowest point of forming limit curve in theory and that in experiment, the maximum shear stress in theory needs to be modified according to the lowest strain of experiment. The maximum shear stress and the required FLD are recorded. Then the related equations are necessary, and the calculation process of the modified shear failure criterion is shown in Figure 2.

(1) The yield function (the same as constitutive function).

(2) The obtained shear stress from the Nonlinear Function (equals to the maximum shear stress).

(3) The strain ratio of Direction 1 and Direction 2 (equals to a given ratio [19], and the ratio is not a constant).

In Figure 2, the deformation process is from zero and the increment of $\Delta\varepsilon_1$ is set as 0.000001. It is found that when the increment of $\Delta\varepsilon_1$ is less than 0.000001, the result will change impossibly. In other words, 0.000001 is small enough for the increment of $\Delta\varepsilon_1$. $\Delta\varepsilon_2$ is calculated with Eq. (6) as shown in Figure 1.

4.2 Experiment Verification

In this part, in order to verify the modified shear failure criterion, two kinds of metals, TRIP780 and 5754O are adopted. The material properties are given from Tables 1, 2, 3, 4, 5, 6. Moreover, the material property parameters, the constitutive model coefficients and the experimental data of forming limit for TRIP780 are from Ref. [20]. The properties of 5754O are from Refs. [21, 22].

4.2.1 Experiment Verification of the FLD for TRIP780

For TRIP780, the modified Voce constitutive [23, 24] and Swift constitutive equations are adopted [24]. The mechanical property parameters of TRIP780 are listed in Table 1 [20]. The related parameters are in Table 2 and Table 3. As shown in Figure 3, the two constitutive equations can better fit the stress-strain curve. The equation of the strain-stress relation $\overline{\sigma} = f\left(\overline{\varepsilon}_p\right)$ can be obtained with the experimental results, where $\overline{\varepsilon}_p$ is the equivalent plastic strain, $\overline{\sigma}$ is the equivalent stress and σ_0 is the initial yield stress [25–27]. The rolling direction is selected as the reference direction. The modified Voce constitutive model is shown in Eq. (29), where A, B, C, D are all constant of the material needed to be fitted with experiment data so as to better describe the deformation process.

$$\overline{\sigma} = A - B\exp\left(-C\overline{\varepsilon}_p\right) + D. \tag{29}$$

The Swift constitutive equation is shown in Eq. (30), where K is the coefficient of material and n is the hardening coefficient of material, which are needed to be fitted with the stress and the strain of material.

$$\overline{\sigma} = K\left(\overline{\varepsilon}_p + \varepsilon_0\right)^n. \tag{30}$$

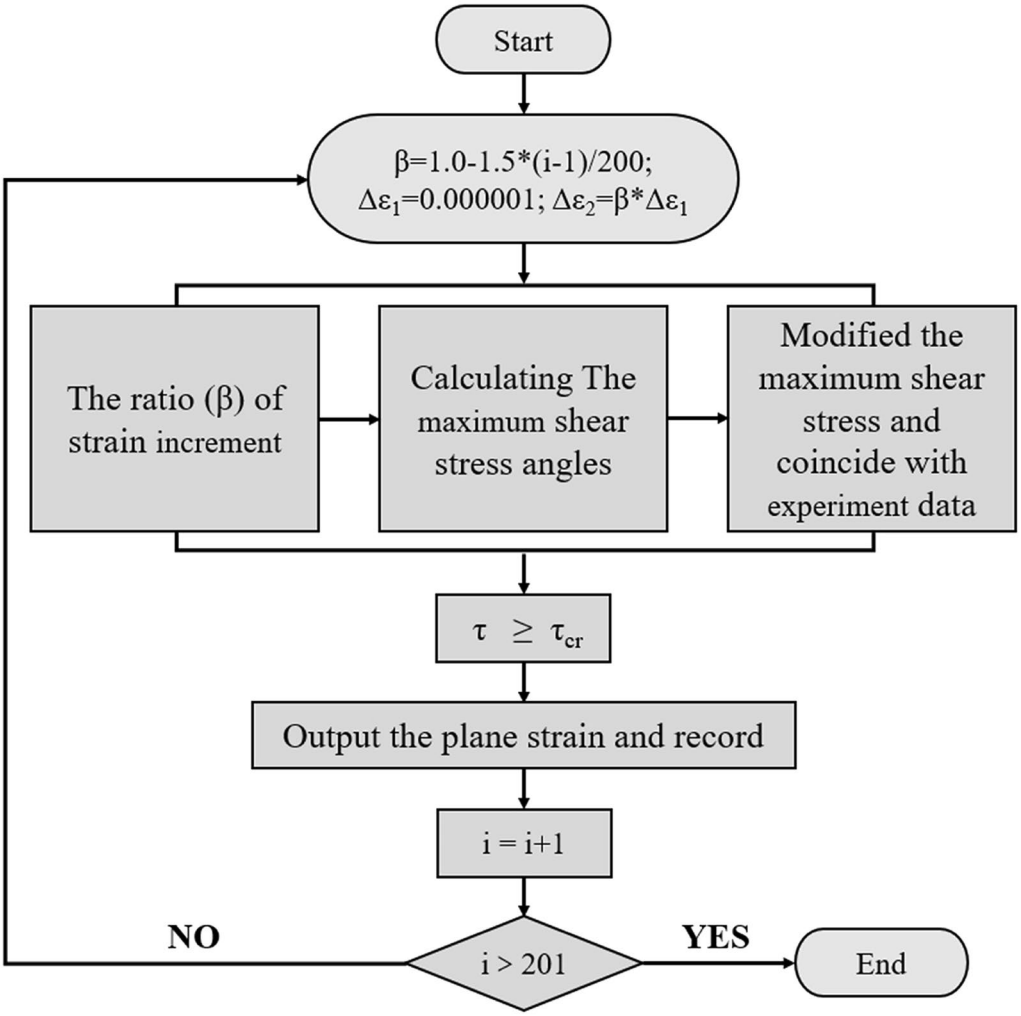

Figure 2 Calculation process of the FLD

Table 1 Mechanical property parameters of TRIP780 [20]

σ_0(MPa)	σ_{45}(MPa)	σ_{90}(MPa)	σ_b(MPa)	r_0	r_{45}	r_{90}
463.5	460.8	497.5	488.1	0.720	0.920	0.830

Table 2 Modified Voce constitutive equation constants of TRIP780 [20]

A	*B*	*C*	*D*
910	479.9	14.240	334.788

Table 3 Swift constitutive equation parameters of TRIP780 [20]

K	*n*	ε_0
1503.6	0.273	0.0083

Based on the modified shear failure criterion proposed above, the FLDs of the TRIP780 under proportional loading path are solved and shown in Figures 4 and 5 with the modified Voce and the Swift constitutive criterion. The FLDs based the original shear failure criterion are also calculated for comparison.

The FLDs of TRIP780, based on the modified Voce constitutive equation in Figure 4 and the Swift constitutive equation in Figure 5, calculated by the original shear failure criterion and the modified shear failure criterion,

Table 4 Mechanical property parameters of 5754O [21]

σ_0(MPa)	σ_{45}(MPa)	σ_{90}(MPa)	σ_b(MPa)	r_0	r_{45}	r_{90}
108.671	108.678	113.385	110.041	0.707	0.894	0.956

Table 5 Swift constitutive equation parameters of 5754O [21]

K	n	ε_0
474.9	0.3236	0.0068

Table 6 Modified swift constitutive equation parameters of 5754O [21]

K	n	ε_0	C
637.8	0.1602	0.0086	− 219.6

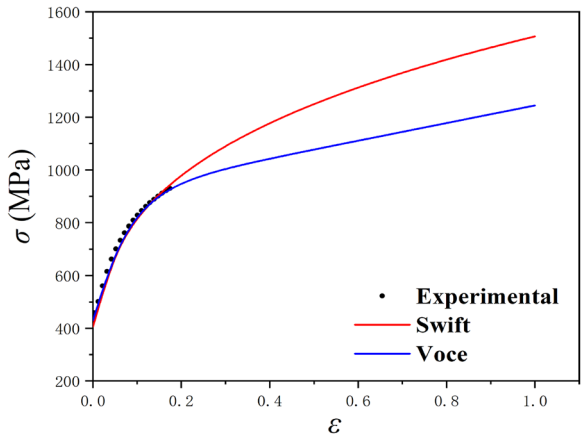

Figure 3 Stress-strain curves of material TRIP780

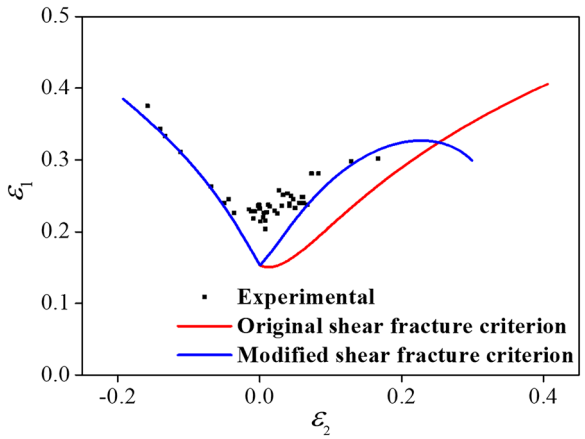

Figure 4 Experimental and theoretical FLD of material TRIP780 based on Modified Voce constitutive equation

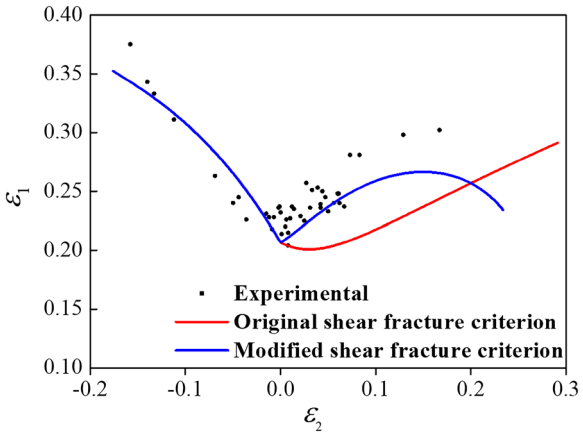

Figure 5 Experimental and theoretical FLD of material TRIP780 based on swift constitutive equation

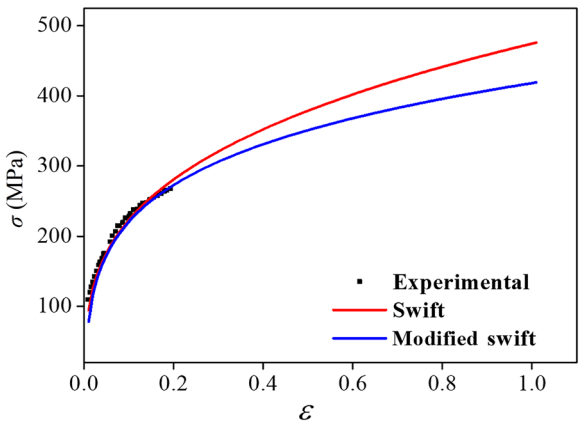

Figure 6 Stress-strain curves of material 5754O

show that these left tensile-compression section of the FLDs are very close. But there are obvious differences in the right part of FLD and the curves based on the modified shear failure criterion are more close to the experiment results. In addition, the forming limit curves calculated with Swift constitutive equation are more close to the experiment results than those with modified Voce equation though the two constitutive equations have the same accuracy for the uniaxial tension as shown in Figure 3.

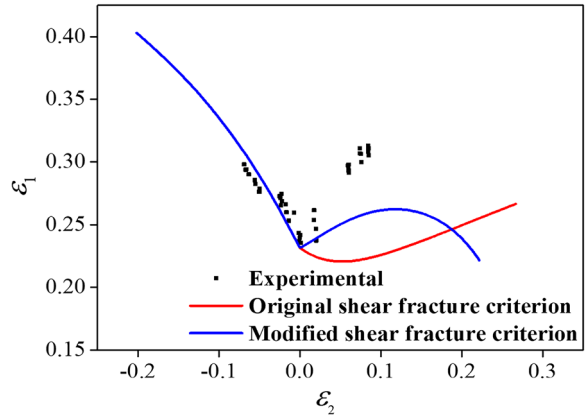

Figure 7 Experimental and theoretical FLD of material 5754O based on Swift constitutive equation

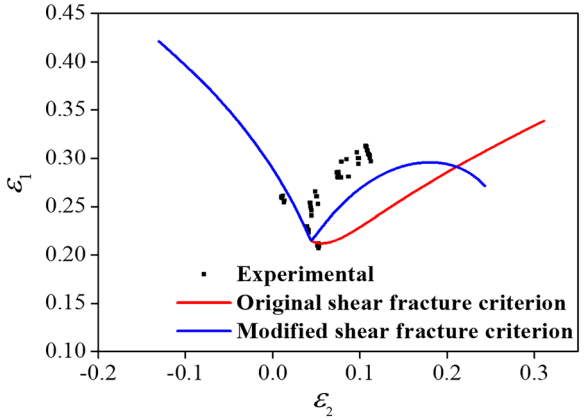

Figure 9 Experimental and theoretical FLD of material 5754O based on modified swift constitutive equation (pre-strain = 0.072, = 0.044)

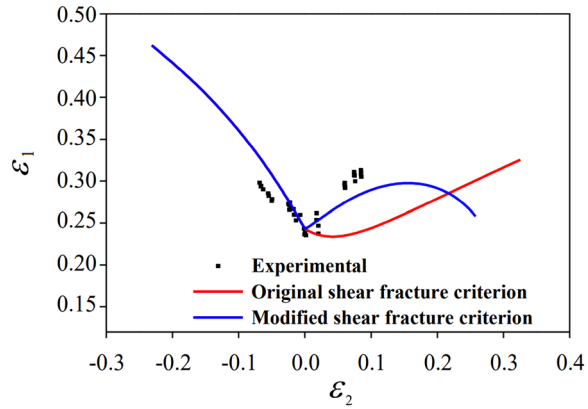

Figure 8 Experimental and theoretical FLDs of material 5754O based on modified swift constitutive equation

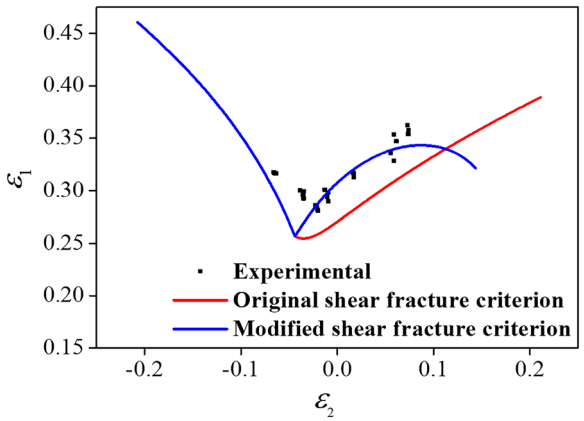

Figure 10 Experimental and theoretical FLD of material 5754O based on modified swift constitutive equation (pre-strain = 0.134, =−0.044)

4.2.2 Experiment Verification of the FLD for 5754O

The mechanical property parameters of 5754O are listed in Table 4. The Swift constitutive model shown in Eq. (30) and the modified Swift constitutive model shown in Eq. (31) are adopted. The related parameters are as shown in Tables 5 and 6. As shown in Figure 6, both of the two constitutive equations can predict the uniaxial tensile properties reasonably.

Compared with Swift constitutive model, the modified Swift constitutive model is shown in Eq. (31), where K is the coefficient of the material, n is the hardening coefficient of material, and C is a constant coefficient to adjust the trends of the FLC, which are needed to be determined with the experiment.

$$\overline{\sigma} = K\left(\overline{\varepsilon}_p + \varepsilon_0\right)^n + C. \tag{31}$$

The FLDs under proportional loading path based on different constitutive equations are shown from Figure 7 and Figure 8 where the experimental data are the same. Under the modified shear failure criterion which shown in Figure 7 and Figure 8 for proportional loading, the FLDs of 5754O based on Swift constitutive equation and the modified Swift constitutive equation are closer to the experimental result than those based on the original shear failure criterion. In addition, the modified Swift constitutive equation has higher accuracy than Swift constitutive equation in predicting FLD based on the proposed shear failure criterion. As Figure 6 shows, although the original and modified swift constitutive equation can describe the uniform deformation, they will bifurcate gradually with deformation becomes larger. The strain value in FLD is obviously larger than that during the uniform process, so that the constitutive equation will affect the prediction of forming limit.

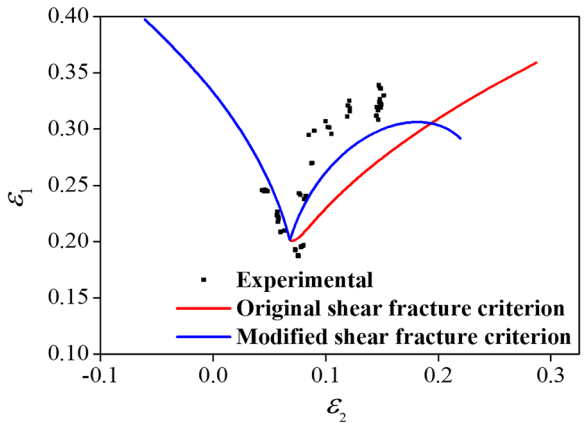

Figure 11 Experimental and theoretical FLD of material 5754O based on modified swift constitutive equation (pre-strain = 0.140, = 0.068)

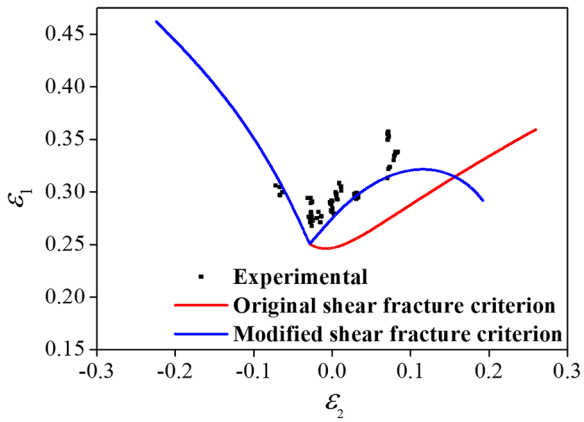

Figure 12 Experimental and theoretical FLD of material 5754O based on modified swift constitutive equation (pre-strain = 0.071, =−0.029)

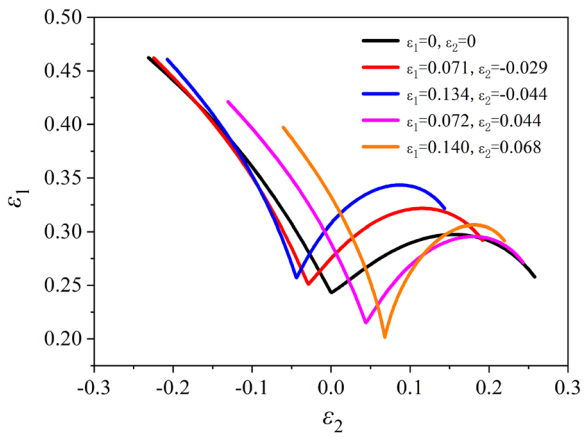

Figure 13 Experimental FLD of material 5754O based on modified shear fracture criterion with modified swift constitutive equation

As shown from Figures 9, 10, 11, 12, the FLDs are under complex loading paths (the FLDs under linear loading path after some pre-strains) based on the modified Swift constitutive equation. From Figures 9, 10, 11, 12, it is shown that the proposed modified shear failure criterion can predict the FLDs more accurate than the original shear failure criterion. As for Figure 11, although the modified shear failure criterion and the modified Swift equation are adopted, there is still deviation between the theoretical and experimental results. There are two possible reasons for this. One is the experimental error and the other is the modified shear failure criterion itself.

The predicted FLDs under linear and complex loading paths based on the modified shear failure criterion are compared in Figure 13. It is found that when the complex pre-strain is close to the uniaxial pre-strain, the forming properties of the material will improve and the forming limit curve will increase. When the complex pre-strain is close to the equal biaxial tensile condition, the forming properties of the material will decrease and the forming limit curve will be lower.

5 Conclusions

(1) The modified shear failure criterion is established in this study. Compared to experimental FLDs of TRIP780 and 5754O, it is shown that the modified shear failure criterion has higher accuracy than original shear failure criterion. With the original criterion, the FLCs trends of the right part of the FLD rise, namely the slope is positive. But with the modified method, the FLCs trends of the right part of the FLD rise firstly and then decline, namely the slope increases firstly and then decreases.

(2) Besides the shear failure criterion, the constitutive equation has obvious effect on the prediction of forming limits. The Swift constitutive equation has high accuracy for TRIP780 steel while the modified Swift constitutive relation fits for 5754 aluminum alloy.

(3) For the forming limits of 5754O with different pre-strains based on the modified shear failure criterion, the FLCs move to the left part of FLD under pre-strain close to uniaxial tension compared with the FLC with no pre-strain. Meanwhile, the FLCs will move to the right part of FLD under the pre-strain close to biaxial tension compared with FLC with no pre-strain.

(4) Although the proposed modified model can predict FLD more accurately than original shear failure criterion, there is still some deviation between the experimental and theoretical data. There are maybe

two reasons for this. The first is that the experimental measurement errors of forming limit data is inevitable. The second is that the loading paths (proportional loading or complex loading) during the theoretical calculation process are ideal, which are not completely coincide with those in experimental process. For instance, for the forming limit experiments under proportional loading path, the stress loading path is difficult to be completely proportional because of the errors from the equipment and tools.

Acknowledgements
The authors sincerely thanks to Mr. Xianzhao Deng for his discussion during manuscript preparation.

Author's Contributions
HW brought forward the main innovative idea: the modified model; YY carried out the deduction and the analysis; ZW was the major contributor in writing the manuscript; YX carried out the calculation. All authors read and approved the final manuscript.

Authors' Information
Haibo Wang, born in 1980, is currently a professor at *North China University of Technology, China*. He received his PhD degree from *Beihang Universtiy, China*, in 2009. His research interests include mechanical engineering, advanced forming technology, constitutive modeling.
Zipeng Wang, born in 1998, is currently a master candidate at *Lab for Materials Forming Mechanism Processes and Equipments, North China University of Technology, China*.
Yu Yan, born in 1983, is currently an associate professor at *North China University of Technology, China*. She received her PhD degree from *Beihang Universtiy, China*, in 2010. Her research interests include mechanical engineering, advanced forming technology, forming process simulation and optimization.
Yuanhui Xu, born in 1990, is currently a master candidate at *Lab for Materials Forming Mechanism Processes and Equipments, North China University of Technology, China*.

Funding
Supported by R&D Program of Beijing Municipal Education Commission of China (Grant No. KZ200010009041), Beijing Municipal University Youth Top Talents Training Program of China (Grant No. CIT&TCD201704014) and Natural Science Foundation of China (Grant No. 51475003).

Declarations

Competing Interests
The authors declare no competing financial interests.

Received: 20 November 2021 Revised: 16 September 2023 Accepted: 22 September 2023
Published online: 31 October 2023

References

[1] F Han, M Wan, X D Wu. Theoretical and experimental investigation progress on the forming limit of sheet metal forming. *Journal of Plasticity Engineering*, 2006, 5: 80-86.
[2] X Huang, J Chen. Review on fracture criterion of sheet metal forming. *Journal of Mechanical Engineering*, 2011, 47(4): 23-31.
[3] R Hill. On discontinuous plastic states with special reference to localized necking in thin sheets. *Journal of the Mechanics and Physics of Solid*, 1952, 1: 19-30.
[4] H W Swift. Plastic instability under plane stress. *Journal of the Mechanics and Physics of Solid*, 1952, 1: 1-18.
[5] Z Marciniak, K Kuczynski. Limit strain in the processes of stretch-forming sheet metal. *International Journal of Mechanical Sciences*, 1967, 9(9): 609-620.
[6] G Chen, S Hu. New concept of forming limit curve. *Journal of Mechanical Engineering,* 1994, 30(2): 82-86
[7] O Björklund, R Larsson, L Nilsson. Failure of high strength steel sheets: Experiments and modeling. *Journal of Materials Processing Technology*, 2017, 213(7): 1103-1117.
[8] Y Lou, J W Yoon, H Huh. Modeling of shear ductile fracture considering a changeable cut-off value for stress triaxiality. *International Journal of Plasticity*, 2014, 54: 56-80.
[9] N Park, H Huh, S J Lim, et al. Fracture-based forming limit criteria for anisotropic materials in sheet metal forming. *International Journal of Plasticity*, 2017, 96: 1-35.
[10] R Deb, J Patrick. Finite volume-based modeling of flow-induced shear failure along fracture manifolds. *International Journal for Numerical and Analytical Methods in Geomechanics*, 2017, 41: 1922-1942.
[11] L T Li, Z H Wang, Z Q Li, et al. *Study on plastic instability behavior of Ti-6Al-4V alloy under composite stress loading*. Harbin: National Conference on Solid Mechanics, 2018.
[12] Y Lou, J W Yoon. Alternative approach to model ductile fracture by incorporating anisotropic yield function. *International Journal of Solids and Structures*, 2019, 164: 12-24.
[13] Y Lou, S Zhang, J W Yoon. Strength modeling of sheet metals from shear to plane strain tension. *International Journal of Plasticity*, 2020, 134: 102813.
[14] Y Lou, S Zhang, J W Yoon. A user-friendly anisotropic ductile fracture criterion for sheet metal under proportional loading. *International Journal of Solids and Structures*, 2021, 217: 48-59.
[15] J Lin, L C Chan, L Wang. Prediction of forming limit diagrams based on shear failure criterion. *International Journal of Solids and Structures*, 2010, 47(21): 2855-2865.
[16] H B Wang, M Wan, Y Yan. Effect of the solving method of parameters on the description ability of the yield criterion about the anisotropic behavior. *Journal of Mechanical Engineering*, 2013, 24: 45-53.
[17] R Hill. A theory of the yielding and plastic flow of anisotropic metals. *Proceedings of the Royal Society of London*, 1948, 193: 281-297.
[18] O Cazacu, F Barlat. Generalization of Drucker's yield criterion to orthotropy. *Mathematics and Mechanics of Solids*, 2001, 6: 613-630.
[19] M Kawka, A Makinouchi. Plastic anisotropy in FEM analysis using degenerated solid element. *Journal of Materials Processing Technology*, 1996, 60: 239-242.
[20] D Anderson, C Butcher, M Worswick. Prediction of edge failure of dual phase 780 steel subjected to hole expansion. *The 9th International Conference and Workshop on Numerical Simulation of 3D Sheet Metal Forming Processes,* Melbourne, Australia, 2013.
[21] H B Wang, M Wan, Y Yan. Effect of flow stress-strain relation on forming limit of 5754O aluminum alloy. *Transactions of Nonferrous Metals Society of China*, 2012, 22: 2370−2378.
[22] H B Wang, Y Yan, F Han, et al. Experimental and theoretical investigations of the forming limit of 5754O aluminum alloy sheet under different combined loading paths. *International Journal of Mechanical Sciences*, 2017, 133: 147-166.
[23] H B Wang, M Wan, X D Wu, et al. Forming limit of sheet metals based on different hardening models. *Journal of Mechanical Engineering*, 2007, 8: 60-65.
[24] S K Kang, Y C Kim, K H Kim, et al. Constitutive equations optimized for determining strengths of metallic alloys. *Mechanics of Materials*, 2014, 73: 51-57.
[25] R Xiao, X X Li, LH Lang, et al. Forming limit in thermal cruciform biaxial tensile testing of titanium alloy. *Journal of Materials Processing Technology*, 2016, 240: 354-361.
[26] X Song, L Leotoing, D Guines, et al. Investigation of the forming limit strains at failure of AA5086 sheets using an in-plane biaxial tensile test. *Engineering Failure Mechanics*, 2016, 163: 130-140.
[27] L Leotoing, D Guines. Investigations of the effect of strain path changes on forming limit curves using an in-plane biaxial tensile test. *International Journal of Mechanical Sciences*, 2015, 99: 21-28.